Recent Advances in Quasi-Poloidal Stellarator Physics Issues

D. A. Spong 1), S. P. Hirshman 1), J. F. Lyon 1), L. A. Berry 1), D. J. Strickler 1), A. S. Ware 2), D. Mikkelsen 3), D. Monticello 3)

1) Oak Ridge National Laboratory, Oak Ridge, TN 37830-6169, U. S. A.
2) University of Montana, Missoula, MT 59812, U. S. A.
3) Princeton Plasma Physics Laboratory, Princeton, NJ, 08543-0451 U. S. A.

Email contact of main author: spongda@ornl.gov

Abstract. The quasi-poloidal stellarator (QPS) hybrid has been developed using a stellarator optimization approach that has proven to be compatible with low aspect ratio. This design includes a number of physics features that are of importance in the development of advanced toroidal devices. These include neoclassical transport levels significantly reduced relative to anomalous, low neoclassical poloidal flow damping rates, reduced bootstrap current levels (relative to the tokamak) that are compatible with steady-state operation, and ballooning second stable regimes. Recent QPS physics research has focused on the calculation of self-consistent plasma flows and the development of physics flexibility scenarios utilizing variable coil and plasma currents. A moments-based analysis has verified that the quasi-symmetry in QPS is sufficient so as to lead to significantly reduced poloidal plasma viscosity. The resulting flux surface averaged plasma flows are dominantly in the poloidal direction with radial shearing. As a result of the low aspect ratio, there is also significant shearing in direction and magnitude of these flows within a flux surface. These features may be useful in suppressing ballooning modes as well as shorter scale length turbulence. Substantial flexibility in the variation of QPS physics properties has been demonstrated through the control of modular, vertical, and toroidal magnet coil currents. Both the low collisonality transport and poloidal viscosity can be varied by large factors by appropriate coil current programming. This system can also be used to suppress magnetic islands both through directly targeting residues of the dominant island chains or by tailoring the rotational transform profile to remain between adjacent resonances. Such methods are applicable both to vacuum and finite plasma pressure states.

1. Introduction

Quasi-poloidal stellarators achieve approximate poloidal symmetry in magnetic coordinates through the use of a racetrack shaped magnetic axis and vertically elongated cross-sections in the regions of high toroidal curvature. This form of optimization has proven to be compatible with the design of compact stellarator hybrid systems such as the two-field-period, very low-aspect-ratio [$\langle R\rangle/\langle a\rangle = 2.7$] QPS configuration,[1] as shown in Fig. 1(a). The highest degree of quasi-poloidal symmetry is achieved in the central regions of the plasma, as shown by the $|B|$ contours at $r/\langle a\rangle = 0.25$ in Fig. 1(b).

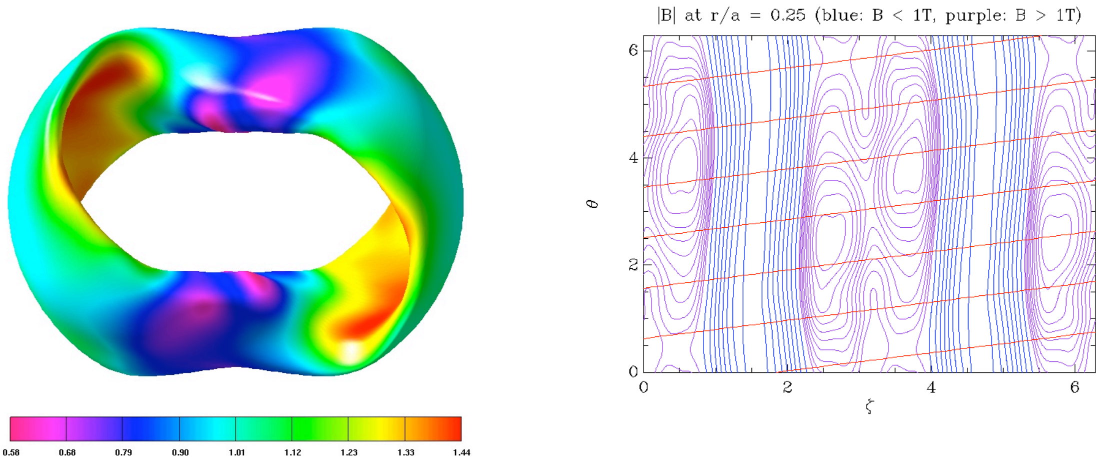

FIG. 1 – (a) Outer magnetic flux surface of QPS showing the magnetic field strength with color contours, (b) Magnetic field strength contours (blue-purple) and magnetic field lines (red) in Boozer coordinates on the flux surface at $(\psi/\psi_{edge})^{1/2}$ =0.25; θ is the poloidal angle variable, and ζ is the toroidal angle variable.

This radial variation in the degree of symmetry is related to the fact that as the magnetic axis is approached, the m > 0 Fourier components of the magnetic field, B_{mn}, decrease to zero, while the m = 0 poloidally symmetric components remain finite. This aspect is also illustrated in Fig. 2(a) where the radial dependence of the ratio of energy in the non-poloidally symmetric B_{mn} modes to that in the symmetric modes is plotted. Fig. 2(b) shows the effective ripple coefficient obtained from the NEO^2 code, which is a measure of low collisionality ripple transport levels. As a result of a comprehensive stellarator optimization process (based on the STELLOPT code), the QPS configuration can achieve similar levels of effective ripple as stellarators with significantly higher aspect ratios while not sacrificing other physics properties.

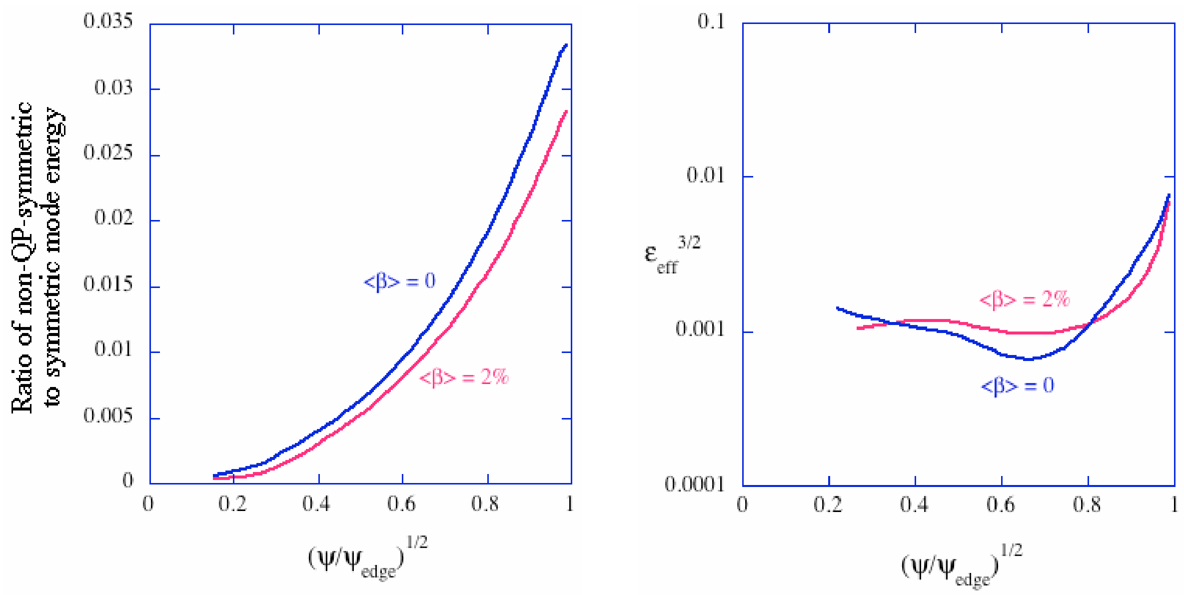

FIG. 2 – (a) Deviation from QP-symmetry as a function of flux surface and <β>, (b) Effective ripple coefficient for QPS as a function of flux surface and <β>.

The larger effective ripple in the outer ~20% of the plasma is not expected to have a strong impact on confinement, due to the more collisional and edge-related transport that will dominate there; it may, in fact, be a desirable feature with respect to the prevention of impurity accumulation. As indicated in the figures, the degree of symmetry and ripple transport is relatively insensitive to changes in the plasma pressure.

2. Moments-Based Method for QPS Transport And Plasma Flows

Plasma flow generation and damping in stellarators is of significance for access to enhanced confinement regimes, impurity transport and magnetic island growth. Unlike the tokamak, where there is a preferred direction (toroidal) for undamped plasma flows, stellarators are characterized by non-zero levels of plasma flow in both toroidal and poloidal directions. The drive mechanisms for stellarator flows also differ from those of tokamaks due to the presence of the ambipolar electric field. A unique feature that distinguishes stellarators with quasi-poloidal symmetry from other toroidal confinement devices, is a lower level of damping for poloidal plasma flows (this possibility was first noted in Ref. 3). In the case of QPS, the relatively low level of externally produced rotational transform ($\iota \approx 0.15$ to 0.25) also implies that the plasma diamagnetic and $E \times B$ flows are oriented in a direction that is close to that (poloidal) in which the viscous damping is minimal. This characteristic is expected to facilitate the generation of sheared plasma flows, which can suppress turbulence and allow the formation of transport barriers.

In order to quantitatively evaluate these features for the QPS device, we have developed a moments-based transport model that takes into account viscous couplings, evaluates the self-consistent electric field, and predicts plasma flow components for stellarators with arbitrary magnetic structure. This method is based upon a recent analysis[4] that formulates stellarator particle and heat flows in terms of viscosities that can in turn be expressed in terms of transport coefficients available from the DKES code.[5] By solving the nonlinear equation obtained from equating the ion and electron particle fluxes, the self-consistent radial electric field can be obtained. The poloidal and toroidal flow components driven by the combined effects of this electric field plus plasma diamagnetic flows can then be derived from the parallel momentum balance relation. We have implemented this procedure in a set of codes that: (a) runs DKES in parallel for each flux surface with subsidiary loops over collisionality and electric field values; (b) extends the resulting computed transport coefficient database to lower collisionality (this is done by matching known asymptotic forms of the transport coefficients to the lowest computed values in the database); (c) converts the DKES coefficients to viscosities and performs the required energy integrations over the mono-energetic coefficients; (d) constructs the coupled ion and electron particle and energy fluxes and solves for the ambipolar electric field; and (e) calculates the plasma flow velocities consistent with the solution obtained for the ambipolar electric field.

We present results based on this model for parameters that are expected to be characteristic of QPS operation in two different heating regimes. For ECH (Electron Cyclotron Heating), a low density, high electron temperature case is used with $n(0) = 2 \times 10^{19}$ m^{-3}, $T_e(0) = 1.8$ keV, $T_i(0) = 0.2$ keV; for ICH (Ion Cyclotron Heating), a higher density $n(0) = 8 \times 10^{19}$ m^{-3}, with $T_e(0) = 0.5$ keV, $T_i(0) = 0.4$ keV is assumed. A broad density profile is used $n(r) = n(0)(1 - 0.2\, r/\langle a\rangle)$ along with parabolic squared profiles for the temperatures (here r denotes an effective minor radius). In the ECH case an electron root (positive electric field) is found while for the ICH case an ion root (negative electric field) is found. Both of these roots are stable against perturbations in the electric field (the sign of $\Gamma_i - \Gamma_e$ is such as to restore[6] the electric field to its equilibrium value). In Fig. 3(a) the self-consistent electric field profiles are plotted based on the applying the above model to the ECH and ICH cases. Results are plotted both as obtained from using the conventional approach where Γ_i and Γ_e are expressed as:

$$\Gamma_{i,e} = -D_{11}^{i,e}\left(\frac{n'_{i,e}}{n_{i,e}} - \frac{3}{2}\frac{T'_{i,e}}{T_{i,e}} - \frac{q_{i,e}E_r}{T_{i,e}}\right) - D_{22}^{i,e}\frac{T'_{i,e}}{T_{i,e}} \tag{1}$$

(the primes denote derivatives with respect to effective minor radius) and using the newer moments-based approach which couples ion and electron flows and frictional forces. Results based on equation (1) are referred to in Fig 3(a) as "without viscous couplings" while those based on the newer method (i.e., Appendix C of ref. 4) are referred to as "with viscous couplings." As can be seen, the moments-based approach generally leads to somewhat larger levels of electric field. In Fig. 3(b) the associated profiles of the flux-surface averaged parallel ion flow velocity are plotted. This velocity is determined by evaluating the parallel momentum balance relation using the self-consistent electric fields of Fig. 3(a). The plasma generates parallel flows that counteract the E × B and diamagnetic driven flow components to the extent necessary to minimize viscous heating.[3] Larger parallel flows are present for the ECH electron root case due to the fact that the electric field and temperature gradients are larger and since the diamagnetic and E × B flows are in the same direction (for ions) whereas they are in opposite directions (partially canceling) for the ICH ion root case.

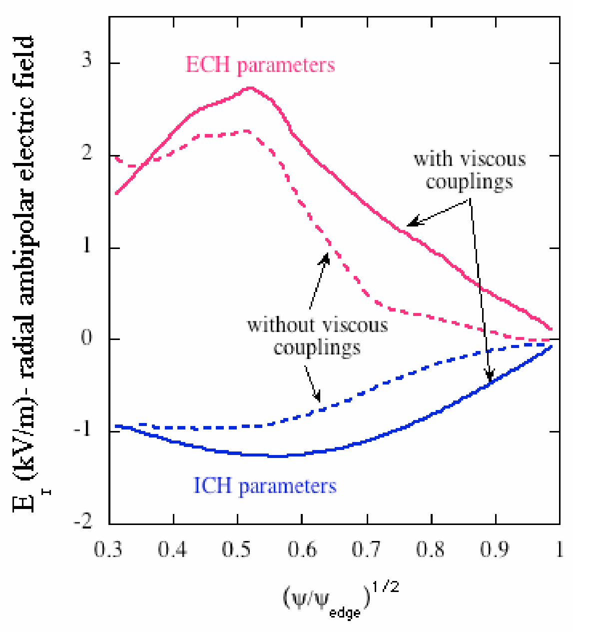

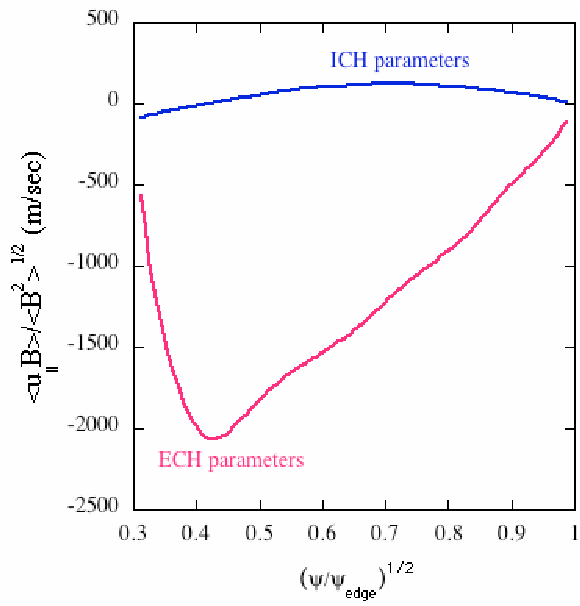

FIG. 3 – (a) Ambipolar electric field vs. flux surface for the ECH and ICH parameters, with and without viscous couplings, (b) Parallel flow velocity vs. flux surface.

Next, it is of interest to examine the partitioning of the flow velocity into poloidal and toroidal components. We first examine the flux-surface averaged form of these velocities, based on the total flow velocity, which is given below:

$$\vec{u} = \frac{X_1}{eB^2}\vec{\nabla} r \times \vec{B} + \left(\frac{\langle u_{\parallel} B \rangle}{\langle B^2 \rangle} + \frac{X_1}{e}\tilde{U} \right)\vec{B}$$

$$\text{where} \quad X_1 = -\frac{1}{n}\frac{dp}{dr} - e\frac{d\phi}{dr} \qquad \text{and } \tilde{U} \text{ satisfies: } \vec{B} \bullet \vec{\nabla}\left(\frac{\tilde{U}}{B}\right) = \vec{B} \times \vec{\nabla} r \bullet \vec{\nabla}\left(B^{-2}\right) \tag{2}$$

This consists of the E × B and diamagnetic components, the parallel flow (as determined from neoclassical parallel momentum balance), and an additional velocity $\tilde{U}$, required to maintain incompressibility. We have calculated the following averages of the flow velocity components:

$$\langle \vec{u} \bullet e^{\theta} \rangle = \left\langle \vec{u} \bullet \frac{\vec{\nabla}\theta}{|\vec{\nabla}\theta|} \right\rangle; \qquad \langle \vec{u} \bullet e^{\zeta} \rangle = \left\langle \vec{u} \bullet \frac{\vec{\nabla}\zeta}{|\vec{\nabla}\zeta|} \right\rangle \tag{3}$$

where the angle brackets denote flux-surface averaging (these differ from the flow velocity components given in Ref. 4 through the use of normalized contra-variant basis vectors). These components are plotted in Fig. 4(a) for the ICH case and Fig. 4(b) for the ECH parameters. As may be seen, the poloidal flow component is strongly dominant in both cases; the velocities reverse signs in going from the ICH to ECH case due to the change in sign of E_r.

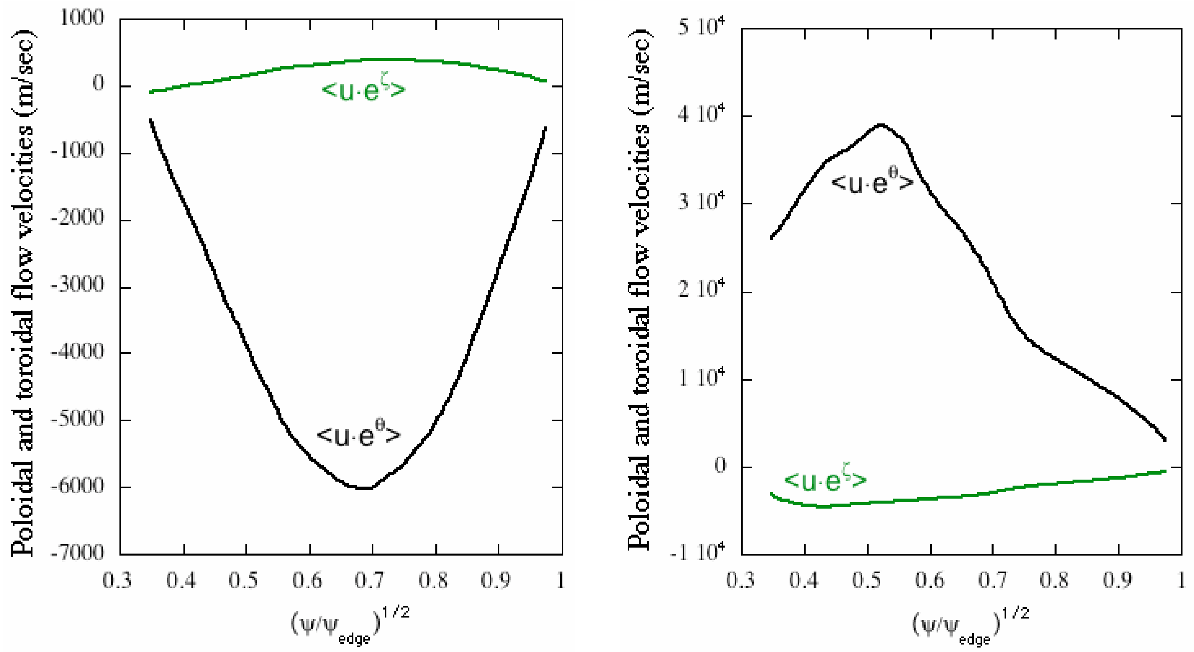

FIG. 4 Flux surface averaged flow velocity components for (a) ICH case and (b) ECH case.

It is also possible to directly display the variation of the flow velocity within a flux surface by transforming the velocity given in Eqn. (2) to Cartesian coordinates and performing 3D renderings as shown in Fig. 5(a) for the ICH parameters and Fig. 5(b) for the ECH parameters. These reveal several interesting aspects of the flow velocity structure that have been suppressed by the flux surface averaging used for the profiles of Fig. 4. In both cases, finite toroidal flow components are present, but these reverse direction in going from the inboard side to the outboard side. This reversal is largely due the impact of the Pfirsh-Schlüter flow component $\tilde{U}$, which is more dominant at low aspect ratios. One can also see that the flows are non-uniform and are especially large in the low field regions of the flux surface [compare to Fig. 1(a)]. This structure is driven simply by the 1/B dependencies of the $E \times B$ and diamagnetic flow terms in Eqn. (2). As a result of these variations, there is considerable velocity shear present within the flux surface, both with respect to the direction of the flow and its magnitude. This flow characteristic may provide an additional mechanism for turbulence suppression in compact stellarators and could also impact ideal and resistive ballooning mode stability.

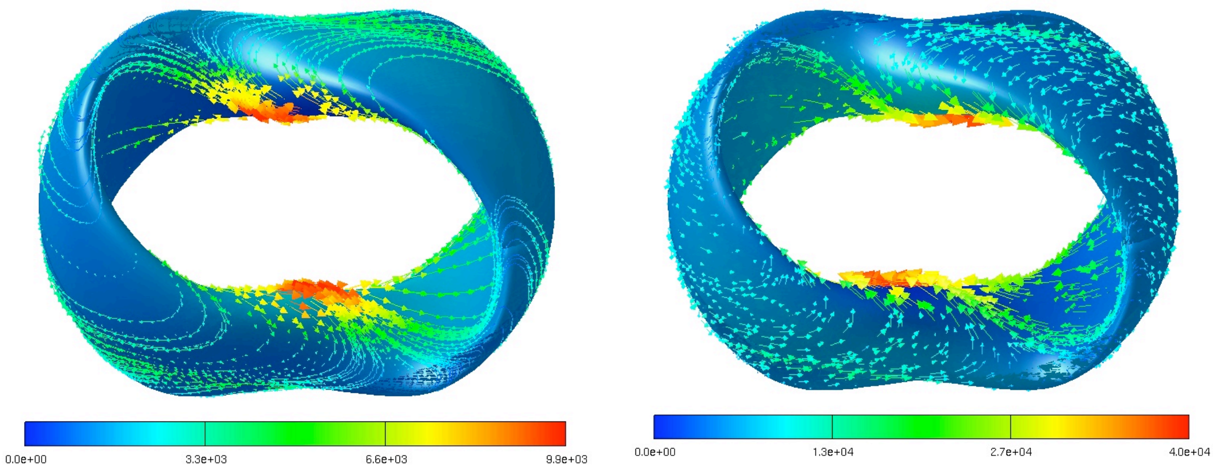

FIG. 5 Variation of the flow velocity within a flux surface for (a) – ICH case and (b) – ECH case.

3. QPS Physics Flexibility Studies

The QPS device will have the capability to vary current levels not only in the vertical and toroidal magnet coils, but also in the plasma and each unique modular coil group. In order to search for extremes in the physics properties accessible through the control of these currents, we have used the merged coil-plasma optimizer code STELLOPT. Large changes in transport coefficients (factor of ~20), quasi-poloidal symmetry (factor of 10), and poloidal viscosity (factor of 10) have been obtained.[7] The effective ripple coefficient,[2] $\varepsilon^{3/2}$ can be varied over a factor of 25-30. This parameter is directly proportional to the low collisionality $1/\nu$ diffusion coefficient through: $D = 2^{3/2}\varepsilon^{3/2}T\rho^2/[9\pi\nu(v)mR^2]$, where T = temperature, ρ = gyroradius, R = major radius, and $\nu(v)$ = energy dependent pitch angle scattering frequency. Fig. 6(a) shows how such variations in effective ripple influence the poloidal viscosity coefficient for the $E_r = 0$ case. In addition, ballooning stability β thresholds can be lowered into ranges that should be accessible by the experiment. Finally, ballooning second stable regimes have been shown to exist[8] in QPS configurations; flexibility in the magnetic structure may be of importance in accessing such high β states.

Variations in coil current distributions have also been useful in controlling field errors and suppressing magnetic islands. As demonstrated in Fig. 6(b), vacuum islands in the QPS device can be suppressed[9] using an optimization strategy that controls modular coil currents so as to minimize the residues[10] of the dominant island chains. We have also minimized island widths both for vacuum and <β> = 2% by using the more conventional technique of targeting of ι profiles that avoid nearby low order resonances. This is achieved through varying both the coil currents and the plasma current. These techniques should provide adequate vacuum island suppression methods and viable startup-up scenarios for access to finite <β> regimes in the QPS device.

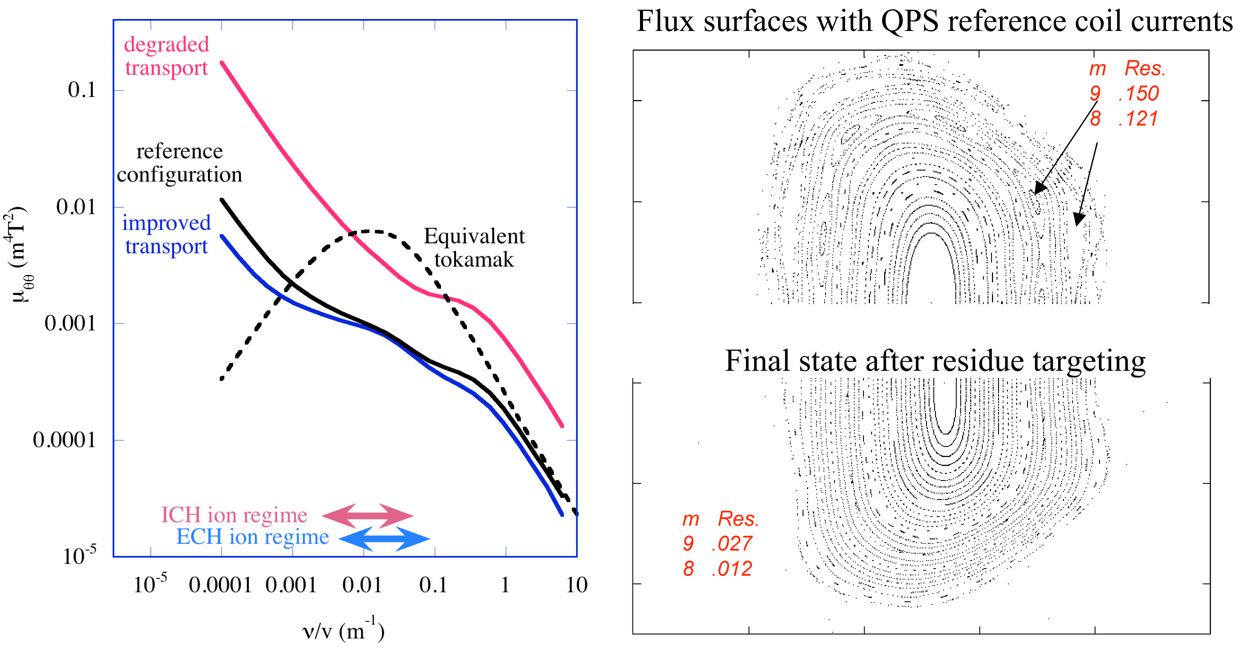

FIG 6 – (a) Poloidal viscosity coefficient at ψ = 0.25 ψ_{edge} for the reference and transport extremized configurations vs. collisionality. (b) Vacuum flux surfaces traced with field line following before (upper) and after (lower) targeting of residues.

4. Conclusions

The QPS approach to stellarator optimization has resulted in a two-field period compact (<R>/<a> = 2.7) design. A sufficient degree of quasi-symmetry has been achieved so as to suppress neoclassical transport losses well below anomalous levels. Recent physics issues that have been of interest for QPS include the analysis of neoclassical plasma flows and exploration of flexibility options that are available when modular, vertical, toroidal magnet coil currents plus plasma currents can be varied. These topics are in addition to ongoing studies of transport, stability, RF heating, and edge physics that have not been discussed here.

Predicted neoclassical plasma flows in QPS have indicated the dominance of the poloidal flow component, as would be expected for this form of quasi-symmetry. This is a unique feature of QP-symmetry and has not been found to the same degree in our studies of tokamaks or other stellarators. It is expected that flows driven by other sources (e.g., turbulence, external sources, etc.) should also experience decreased viscous damping in the poloidal direction. Furthermore, the low aspect ratio of QPS results in a higher degree of flow shearing within a flux surface than present in higher aspect ratio configurations. These characteristics will be investigated further with regard to their impact on microturbulence, and ideal/resistive ballooning modes.

Flexibility studies for QPS have provided encouraging initial results that the transport and stability properties of this device can be varied over significant ranges by varying magnet coil currents (modular, vertical, toroidal). Also, magnetic island suppression has been achieved using both direct island residue targeting as well as controlling the rotational transform profile to remain between adjacent low order rational values.

Acknowledgements - Work supported by U.S. Department of Energy under Contract DE-AC05-00OR22725 with UT-Battelle, LLC.

[1] SPONG, D.A., HIRSHMAN, S. P., BERRY, L. A., LYON, J. F., FOWLER, R. H., STRICKLER, D. J., COLE, M. J., NELSON, B. N., WILLIAMSON, D. E., WARE, A. S., ALBAN, D., SANCHEZ, R., FU, G. Y., MONTICELLO, D. A., MINER, JR., W. H., VALANJU, P. M., Physics Issues of Compact Drift Optimized Stellarators, Nuclear Fusion **41** (2001) 711.
[2] NEMOV, V. V., KASILOV, S. V., KERNBICHLER, W., HEYN, M. F., Phys. Plasmas **6** (1999) 4622.
[3] SHAING, K., CALLEN, J. D., Neoclassical Flows and Transport in Nonaxisymmetric Toroidal Plasmas, Phys. Fluids **26** (1983) 3315.
[4] SUGAMA, H., NISHIMURA, S., How to Calculate the Neoclassical Viscosity, Diffusion, and Current Coefficients in General Toroidal Plasmas, Phys. Plasmas **9** (2002) 4637.
[5] VAN RIJ, W. I., HIRSHMAN, S. P., Variational Bounds for Transport Coefficients in Three-Dimensional Toroidal Plasmas, Phys. Fluids B **1** (1989) 563.
[6] SHAING, K. C., Stability of the Electric Field in a Nonaxisymmetric Torus, Phys. Fluids **27** (1984) 1567; also, JAEGER, E. F., SPONG, D. A., HEDRICK, C. L., Phys. Rev. Lett. **40** (1978) 866.
[7] SPONG, D. A., STRICKLER, D.J., HIRSHMAN, S.P., ET AL., QPS Transport Physics Flexibility Using Variable Coil Currents, Fusion Science and Technology **46** (2004) 215.
[8] Ware, A. S., Hirshman, S. P., Spong, D. A., Berry, L. A., Deisher, A. J., Fu, G. Y., Lyon, J. F., Sanchez, R., "High-Beta Equilibria of Drift-Optimized Compact Stellarators," Phys. Rev. Lett. **89** (2002) 125003-1.
[9] STRICKLER, D.J., HIRSHMAN, S.P., SPONG, D.A., COLE, M.J., LYON, J.F., NELSON, B.E., WILLIAMSON, D.E. AND WARE, A.S., Development of a Robust Quasi-Poloidal Compact Stellarator, Fusion Science and Technology **45** (2004) 15.
[10] CARY, J., HANSON, J., Phys. Fluids **29** (1986) 2464.